Broadband MIMO-OFDM Wireless Communications

GORDON L. STÜBER, FELLOW, IEEE, JOHN R. BARRY, MEMBER, IEEE,
STEVE W. MCLAUGHLIN, SENIOR MEMBER, IEEE, YE (GEOFFREY) LI, SENIOR MEMBER, IEEE,
MARY ANN INGRAM, SENIOR MEMBER, IEEE, AND THOMAS G. PRATT, MEMBER, IEEE

Invited Paper

Orthogonal frequency division multiplexing (OFDM) is a popular method for high data rate wireless transmission. OFDM may be combined with antenna arrays at the transmitter and receiver to increase the diversity gain and/or to enhance the system capacity on time-variant and frequency-selective channels, resulting in a multiple-input multiple-output (MIMO) configuration. This paper explores various physical layer research challenges in MIMO-OFDM system design, including physical channel measurements and modeling, analog beam forming techniques using adaptive antenna arrays, space–time techniques for MIMO-OFDM, error control coding techniques, OFDM preamble and packet design, and signal processing algorithms used for performing time and frequency synchronization, channel estimation, and channel tracking in MIMO-OFDM systems. Finally, the paper considers a software radio implementation of MIMO-OFDM.

Keywords*—Adaptive antennas, broadband wireless, multiple-input multiple-output (MIMO), orthogonal frequency division multiplexing (OFDM), software radio, space–time coding, synchronization.*

I. INTRODUCTION

Orthogonal frequency division multiplexing (OFDM) has become a popular technique for transmission of signals over wireless channels. OFDM has been adopted in several wireless standards such as digital audio broadcasting (DAB), digital video broadcasting (DVB-T), the IEEE 802.11a [1] local area network (LAN) standard and the IEEE 802.16a [2] metropolitan area network (MAN) standard. OFDM is also being pursued for dedicated short-range communications (DSRC) for road side to vehicle communications and as a potential candidate for fourth-generation (4G) mobile wireless systems.

Manuscript received June 23, 2003; revised November 3, 2003. This work was supported in part by the Yamacraw Mission (http://www.yamacraw.org) and in part by the National Science Foundation under Grant CCR-0121565.

The authors are with the School of Electrical and Computer Engineering, Georgia Institute of Technology, Atlanta, GA 30332 USA.

Digital Object Identifier 10.1109/JPROC.2003.821912

OFDM converts a frequency-selective channel into a parallel collection of frequency flat subchannels. The subcarriers have the minimum frequency separation required to maintain orthogonality of their corresponding time domain waveforms, yet the signal spectra corresponding to the different subcarriers overlap in frequency. Hence, the available bandwidth is used very efficiently. If knowledge of the channel is available at the transmitter, then the OFDM transmitter can adapt its signaling strategy to match the channel. Due to the fact that OFDM uses a large collection of narrowly spaced subchannels, these adaptive strategies can approach the ideal water pouring capacity of a frequency-selective channel. In practice this is achieved by using adaptive bit loading techniques, where different sized signal constellations are transmitted on the subcarriers.

OFDM is a block modulation scheme where a block of N information symbols is transmitted in parallel on N subcarriers. The time duration of an OFDM symbol is N times larger than that of a single-carrier system. An OFDM modulator can be implemented as an inverse discrete Fourier transform (IDFT) on a block of N information symbols followed by an analog-to-digital converter (ADC). To mitigate the effects of intersymbol interference (ISI) caused by channel time spread, each block of N IDFT coefficients is typically preceded by a cyclic prefix (CP) or a guard interval consisting of G samples, such that the length of the CP is at least equal to the channel length. Under this condition, a linear convolution of the transmitted sequence and the channel is converted to a circular convolution. As a result, the effects of the ISI are easily and completely eliminated. Moreover, the approach enables the receiver to use fast signal processing transforms such as a fast Fourier transform (FFT) for OFDM implementation [3]. Similar techniques can be employed in single-carrier systems as well, by preceding each transmitted data block of length N by a CP of length G, while using frequency-domain equalization at the receiver.

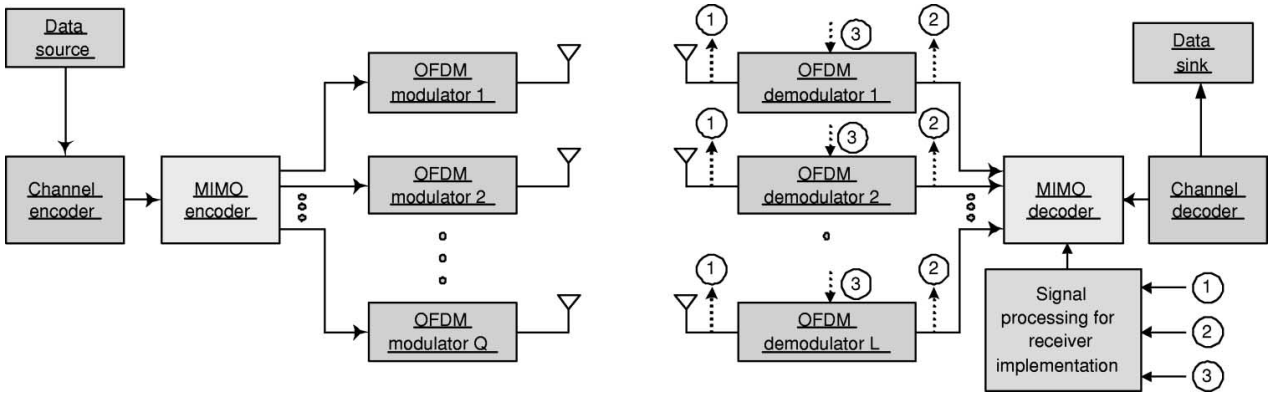

Fig. 1. $Q \times L$ MIMO-OFDM system, where Q and L are the numbers of inputs and outputs, respectively.

Multiple antennas can be used at the transmitter and receiver, an arrangement called a multiple-input multiple-output (MIMO) system. A MIMO system takes advantage of the spatial diversity that is obtained by spatially separated antennas in a dense multipath scattering environment. MIMO systems may be implemented in a number of different ways to obtain either a diversity gain to combat signal fading or to obtain a capacity gain. Generally, there are three categories of MIMO techniques. The first aims to improve the power efficiency by maximizing spatial diversity. Such techniques include delay diversity, space–time block codes (STBC) [4], [5] and space–time trellis codes (STTC) [6]. The second class uses a layered approach to increase capacity. One popular example of such a system is V-BLAST suggested by Foschini *et al.* [7] where full spatial diversity is usually not achieved. Finally, the third type exploits the knowledge of channel at the transmitter. It decomposes the channel coefficient matrix using singular value decomposition (SVD) and uses these decomposed unitary matrices as pre- and post-filters at the transmitter and the receiver to achieve near capacity [8].

OFDM has been adopted in the IEEE802.11a LAN and IEEE802.16a LAN/MAN standards. OFDM is also being considered in IEEE802.20a, a standard in the making for maintaining high-bandwidth connections to users moving at speeds up to 60 mph. The IEEE802.11a LAN standard operates at raw data rates up to 54 Mb/s (channel conditions permitting) with a 20-MHz channel spacing, thus yielding a bandwidth efficiency of 2.7 b/s/Hz. The actual throughput is highly dependent on the medium access control (MAC) protocol. Likewise, IEEE802.16a operates in many modes depending on channel conditions with a data rate ranging from 4.20 to 22.91 Mb/s in a typical bandwidth of 6 MHz, translating into a bandwidth efficiency of 0.7 to 3.82 bits/s/Hz. Recent developments in MIMO techniques promise a significant boost in performance for OFDM systems. Broadband MIMO-OFDM systems with bandwidth efficiencies on the order of 10 b/s/Hz are feasible for LAN/MAN environments. The physical (PHY) layer techniques described in this paper are intended to approach 10 b/s/Hz bandwidth efficiency.

This paper discuss several PHY layer aspects broadband MIMO-OFDM systems. Section II describes the basic MIMO-OFDM system model. All MIMO-OFDM receivers must perform time synchronization, frequency offset estimation, and correction and parameter estimation. This is generally carried out using a preamble consisting of one or more training sequences. Once the acquisition phase is over, receiver goes into the tracking mode. Section III provides an overview of the signal acquisition process and investigates sampling frequency offset estimation and correction in Section IV. The issue of channel estimation is treated in Section V. Section VI considers space–time coding techniques for MIMO-OFDM, while Section VII discusses coding approaches. Adaptive analog beam forming approaches can be used to provide the best possible MIMO link. Section VIII discusses various strategies for beamforming. Section IX very briefly considers medium access control issues. Section X discusses a software radio implementation for MIMO-OFDM. Finally, Section XI wraps up with some open issues concluding remarks.

II. MIMO-OFDM System Model

A multicarrier system can be efficiently implemented in discrete time using an inverse FFT (IFFT) to act as a modulator and an FFT to act as a demodulator. The transmitted data are the "frequency" domain coefficients and the samples at the output of the IFFT stage are "time" domain samples of the transmitted waveform. Fig. 1 shows a typical MIMO-OFDM implementation.

Let $\mathbf{X} = \{X_0, X_1, \ldots, X_{N-1}\}$ denote the length-N data symbol block. The IDFT of the date block $\mathbf{X}$ yields the time domain sequence $\mathbf{x} = \{x_0, x_1, \ldots, x_{N-1}\}$, i.e.,

$$x_n = \text{IFFT}_N\{X_k\}(n). \tag{1}$$

To mitigate the effects of channel delay spread, a guard interval comprised of either a CP or suffix is appended to the sequence $\mathbf{X}$. In case of a CP, the transmitted sequence with guard interval is

$$x_n^g = x_{(n)_N},\ n = -G, \ldots, -1, 0, 1, \ldots, N-1 \tag{2}$$

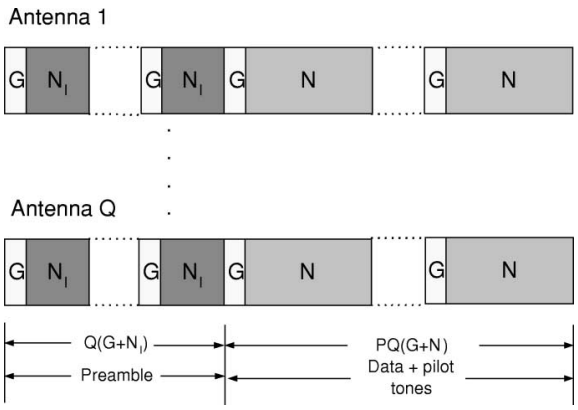

Fig. 2. Frame structure for the $Q \times L$ OFDM system.

where G is the guard interval length in samples, and $(n)_N$ is the residue of n modulo N. The OFDM complex envelope is obtained by passing the sequence $\mathbf{x}^g$ through a pair of ADCs (to generate the real and imaginary components) with sample rate $1/T$ s, and the analog I and Q signals are upconverted to an RF carrier frequency. To avoid ISI, the CP length G must equal or exceed the length of the discrete-time channel impulse response M. The time required to transmit one OFDM symbol $T_s = NT + GT$ is called the OFDM symbol time. The OFDM signal is transmitted over the passband RF channel, received, and downconverted to base band. Due to the CP, the discrete linear convolution of the transmitted sequence with the channel impulse response becomes a circular convolution. Hence, at the receiver the initial G samples from each received block are removed, followed by an N-point discrete Fourier transform (DFT) on the resulting sequence.

The frame structure of a typical MIMO-OFDM system is shown in Fig. 2. The OFDM preamble consists of Q training symbols of length N_I+G, where $G \leq N_I \leq N$, $N_I = N/I$ and I an integer that divides N. Often the length of the guard interval in the training period is doubled; for example, in IEEE802.16a [1], to aid in synchronization, frequency offset estimation and equalization for channel shortening in cases where the length of the channel exceeds the length of the guard interval.

First consider the preamble portion of the OFDM frame. The length-$N_I + G$ preamble sequences are obtained by exciting every Ith coefficient of a length-N frequency-domain vector with a nonzero training symbol from a chosen alphabet (the remainder are set to zero). The frequency-domain training sequences transmitted from the ith antenna are $\{S_k^{(q)}\}_{k=1}^{N}$, where $q = (c-1)Q + i$ and $c = 1, 2, \ldots, Q$ The individual length-N_I time domain training sequences are obtained by taking an N-point IDFT of the sequence $\{S_k^{(q)}\}_{k=1}^{N}$, keeping the first N_I time-domain coefficients and discarding the rest. A CP is appended to each length-N_I time-domain sequence. Let $\mathbf{H}_{ij}$ be the vector of subchannel coefficients between the ith transmit and the jth receive antenna and let $\{R_k^{(l)}\}_{k=0}^{N_I-1}$ be the received sample sequence at the lth receiver antenna. After removing the guard interval, the received samples $\{R_k^{(l)}\}_{k=0}^{N_I-1}$ are repeated I times and demodulated using an N-point FFT as

$$R_k^{(l)} = \mathrm{FFT}_N\{r^{(l)}\}(k) \tag{3}$$

$$= \sum_{q=1}^{Q} H_k^{(q,l)} S_k^{(q)} + W_k^{(l)} \tag{4}$$

where $k = 0, \ldots, N-1$. The demodulated OFDM sample matrix $\mathbf{R}_k$ of dimension $(Q \times L)$ for the kth subcarrier can be expressed in terms of the transmitted sample matrix $\mathbf{S}_k$ of dimension $(Q \times Q)$, the channel coefficient matrix $\mathbf{H}_k$ of dimension $(Q \times L)$ and the additive white Gaussian noise matrix $\mathbf{W}_k$ of dimension $(Q \times L)$ [24] as

$$\mathbf{R}_{k,Q\times L} = \mathbf{S}_{k,Q\times Q} \cdot \mathbf{H}_{k,Q\times L} + \mathbf{W}_{k,Q\times L} \tag{5}$$

where $\mathbf{R}$, $\mathbf{H}$, and $\mathbf{W}$ can viewed as either a collection of N matrices of dimension $Q \times L$ or as a collection of $Q \times L$ vectors of length N.

A. Preamble Design for MIMO-OFDM Systems

Least square channel estimation schemes require that all $Q \times N_I$ training symbol matrices $\mathbf{S}^{(q)}$, $q = (c-1)Q + k$, $k = 1, \ldots, N_I$ be unitary so that only Q OFDM symbols are needed for channel estimation [25]. A straightforward solution is to make each $\mathbf{S}_k$ a diagonal matrix. However, the power of the preamble needs to be boosted by $10 \log_{10} Q$ dB in order to achieve a performance similar to the case when the preamble signal is transmitted from all the antennas. This has the undesirable effect of increasing the dynamic range requirements of the power amplifiers. Hence, methods are required so that sequences can be transmitted from all the antennas while still having unitary $\mathbf{S}_k$ matrices. One approach adapts the work by Tarokh *et al.* on space–time block codes [5], [26]. For $Q = 2$, 4, and 8, orthogonal designs exist. For example, for $Q = 2$ and 4, we can choose the preamble structures of the form

$$\mathbf{S}_{AS} = \begin{bmatrix} \mathbf{S}_1 & \mathbf{S}_1 \\ -\mathbf{S}_1 & \mathbf{S}_1 \end{bmatrix} \tag{6}$$

$$\mathbf{S}_{TS} = \begin{bmatrix} \mathbf{S}_1 & \mathbf{S}_1 & \mathbf{S}_1 & \mathbf{S}_1 \\ -\mathbf{S}_1 & \mathbf{S}_1 & -\mathbf{S}_1 & \mathbf{S}_1 \\ -\mathbf{S}_1 & \mathbf{S}_1 & \mathbf{S}_1 & -\mathbf{S}_1 \\ -\mathbf{S}_1 & -\mathbf{S}_1 & \mathbf{S}_1 & \mathbf{S}_1 \end{bmatrix} \tag{7}$$

where $\mathbf{S_1}$ is the length-N_I vector S_k, $k = 1 \ldots N_I$. This results in unitary $\mathbf{S}_k$ matrices. As it turns out, transmitting the same sequence from all the antennas in this fashion is advantageous when performing synchronization. A similar structure for $Q = 8$ exists. For other values of Q, a least squares (LS) solution for the channel estimates can be obtained by either transmitting more than Q training sequences or by making the training symbol matrices unitary by using a Gram–Schmidt orthonormalization procedure as described in [24].

B. Pilot Insertion

Channel coefficients require constant tracking. This is aided by inserting known pilot symbols at fixed or variable subcarrier positions. For example, the IEEE 802.16a

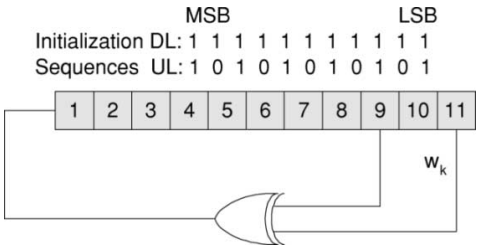

Fig. 3. Pilot tone generation.

standard recommends the insertion of eight pilot tones at fixed positions on subcarriers [12, 36, 60, 84, 172, 196, 220, 244] (assuming $N = 256$). Fig. 3 shows the method for generating the pilot sequences used in the IEEE 802.16a standard. In the downlink (DL) and the uplink (UL), the shift register is initialized with sequences as shown. A 0 at the output P_n is mapped to $+1$ and a 1 is mapped to -1. For a MIMO system with $Q = 2$ and 4 antennas, the pilot sequences p_n can be coded over space and time to form structures in (6) and (7), respectively, thereby admitting a simple LS channel estimate. For more information on the pilot sequence construction, readers can refer to [27].

III. Synchronization in the Acquisition Mode

Time and frequency synchronization can be performed sequentially in the following steps [28].

Step 1) *Coarse Time Synchronization and Signal Detection*—Coarse time acquisition and signal detection locates the start of an OFDM frame over an approximate range of sample values. Due to the presence of the CP (or suffix), coarse time acquisition during the preamble can be performed by correlating the received samples that are at a distance of N_I from each other over a length-G window ([25], [29]), viz.

$$n_{j,\text{coarse}} = \arg \underbrace{\max}_{n} \{\phi_{j,n}\}. \tag{8}$$

where $\phi_{j,n} = \sum_{k=0}^{G-1} (r^*_{j,n+k} \cdot r_{j,n+k+N_I})$. In addition to maximizing $\phi_{j,n}$, it should also exceed a certain threshold to reduce the probability of false alarm (P_{FA}). We chose the threshold to be 10% of the incoming signal energy of the correlation window.

Step 2) *Frequency Offset Estimation in the Time Domain*—Any frequency offset between the transmitter and the receiver local oscillators is reflected in the time domain sequence as a progressive phase shift $\theta = 2\pi\gamma N_I/N$, where γ is the frequency offset and is defined as the ratio of the actual frequency offset to the intercarrier spacing. A frequency offset estimate of up to $\pm I/2$ subcarrier spacings can be obtained based on the phase of the autocorrelation function in (8) as follows:

$$\hat{\gamma}_j = \frac{I}{2\pi} \angle\{\phi_{n_{j,\text{coarse}}}\} \tag{9}$$

where $n_{j,\text{coarse}}$ is the optimum coarse timing acquisition instant and $I = N/N_I$. The frequency offset can then be removed from the received sample sequence by multiplying it with $\exp\{-j2\pi\hat{\gamma}n/N_I\}$ during the preamble and $\exp\{-j2\pi\hat{\gamma}n/N\}$ during the data portion. Note that by reducing the length of the training symbol by a factor of I, the range of the frequency offset estimate in the time domain can be increased by a factor of I.

Step 3) *Residual Frequency Offset Correction*—Should the range of the time domain frequency offset estimation be insufficient, frequency-domain processing can be used. Suppose that the same frequency-domain training sequence $\{S_k^{(q)}\}_{k=1}^N$ is transmitted from all the antennas. The residual frequency offset, that is, an integer multiple of the subcarrier spacing, can be estimated by computing a cyclic cross-correlation of $\{S_k^{(q)}\}_{k=1}^N$ with the received, frequency corrected (from Step II), demodulated symbol sequence, viz.,

$$\chi_k = \sum_{n=0}^{N-1} S^{(q)*}_{(k+n)_N} R^{(1)^c}_n \quad k=0,1,\ldots,N-1 \tag{10}$$

where

$$R^{(1)^c}_n = \text{FFT}_N \left\{ r_n^{(1)} e^{j2\pi\hat{\gamma}_{\text{ML}} n/N_I} \right\}. \tag{11}$$

The residual frequency offset is estimated as $\hat{\Gamma} = \arg\max\{|\chi_k|\}$, $k = 0, 1, \ldots, N-1$. Note that the fractional part of the relative frequency offset is estimated in the time domain in Step II while the integer part is estimated in the frequency domain in Step III.

Step 4) *Fine Time Synchronization*—Fine time acquisition locates the start of the useful portion of the OFDM frame to within a few samples. Once the frequency offset is removed, fine time synchronization can be performed by cross correlating the frequency corrected samples with the transmitted preamble sequences. The fine time synchronization metric is

$$n_{j,\text{fine}} = \arg \underbrace{\max}_{n} \{\psi_{j,n}\} \tag{12}$$

where $\psi_{j,n} = \sum_{q=1}^{Q} \left| \sum_{k=0}^{N_I-1} (s^*_{q,k} \cdot r_{j,n+k}) \right|$. For systems using two and four and eight transmit antennas using the orthogonal designs discussed in Section II-A, only one cross correlator is needed per receiver antenna. Once again the threshold is set at 10% of the energy contained in N_I received samples. Since fine time synchronization is computationally expensive process, it is carried out for a small window centered around the coarse time synch. instant $n_{j,\text{coarse}}$.

Finally, the net time synchronization instant for the entire receiver is selected to be $n_{\text{opt}} = (1/L) \sum_{j=1}^{L} n_{j,\text{fine}}$. An added negative offset of a few samples is applied to the

Table 1
SUI-4 Channel Model

	Tap 1	Tap 2	Tap 3	Units
Delay	0	1.5	4.0	μs
Power (omni ant.)	0	−4	−8	dB
Doppler f_m	0.2	0.15	0.25	Hz

fine time synchronization instant in order to ensure that the OFDM windows for all the receivers falls into an ISI-free zone.

A. Example

Consider a 2×2 and a 4×4 broadband MIMO-OFDM system [2] operating at a carrier frequency of 5.8 GHz on the SUI-4 channel shown in Table 1. The OFDM signal occupies a bandwidth of 4.0 MHz. The uncorrected frequency offset $(\Gamma + \gamma)$ is 1.25 subcarrier spacings. The OFDM blocksize is $N = 256$, and the guard interval is kept at $N/4 = 64$. Out of 256 tones, the dc tone and 55 other tones at the band edges are set to zero. Hence, the number of used tones $N_u = 200$. The length of the sequences used in the preamble is varied from N to $N/2$ to $N/4$. The preamble insertion period P is chosen to be ten. STBCs are used to encode the data. For a 2×2 system, the Alamouti STBC is used with code rate 1, whereas for a 4×4 system, code rate is 3/4 [26]. In the data mode, each of the tones is modulated using a 16-QAM constellation and no channel coding is employed. LS channel estimates obtained using the preamble are used to process the entire frame [28]. For training sequences of length $N_I < N$, frequency-domain linear interpolation and extrapolation are used. Afterwards, frequency-domain smoothing is used, such that channel estimates at the band-edges are kept as they are, whereas all the other channel estimates are averaged using

$$\hat{H}_k^{(q,j)} = \frac{\bar{H}_{k-1}^{(q,j)} + \bar{H}_{k+1}^{(q,j)}}{2}. \tag{13}$$

Fig. 4 shows the coarse and fine time synchronization performance for a 4×4 MIMO-OFDM system with $N_I = 128$, $I = 2$, and signal-to-noise ratio (SNR) of 10 dB.

Fig. 5 shows the overall bit error rate (BER) performance of a 2×2 MIMO-OFDM system using the suggested algorithms.

IV. Sample Frequency Offset Correction and Tracking

MIMO-OFDM schemes that use coherent detection need accurate channel estimates. Consequently, the channel coefficients must be tracked in a system with high Doppler. In the broadband fixed wireless access (BFWA) system IEEE 802.16a, the channel is nearly static. However, channel variations are still expected due to the presence of sampling frequency offset between transmitter and the receiver RF oscillators. Generally, the components in the customer premises equipment (CPE) have a low tolerance with typical drift of 20 parts per million (ppm). This means a signal with a BW of 4 MHz produces an offset of 80 samples for every 1 s of transmission. Sample frequency offset causes phase rotation, amplitude distortion and loss in synchronization.

Even after successful signal acquisition and synchronization, the OFDM system must guard against sample frequency offset (SFO) and phase offset. It must also guard against drift in the RF local oscillator and sampling clock frequency with time [30].

Let $T' \neq T$ be the sampling time at the receiver and let $\beta = (T' - T)/T$ be the normalized offset in the sampling time. The received and demodulated OFDM symbol with the sampling time offset can be approximated by (14), at the bottom of the page. where $k = 0, \ldots, N-1, l = (j-1)Q+g$ and $g = 1, 2, \ldots, Q$ is the running index of the OFDM symbol in time, and $\mathrm{sinc}(x) = \sin(\pi x)/\pi x$.

Due to the sampling frequency offset β, the received demodulated symbol suffers phase rotation as well as amplitude distortion. In general, the value of β is very small. For example, for a sampling clock tolerance of 20 ppm and sampling frequency $f_s = 8$ MHz, $\beta = 2 \times 10^{-5}$. Hence, $\mathrm{sinc}(k\beta) \approx 1$ and its effect is negligible. With this assumption, the demodulated OFDM sample matrix $\mathbf{R}_k$ in (5) becomes

$$\mathbf{R}_{k,Q\times L} = \mathbf{\Lambda}_{k,Q\times Q} \cdot \mathbf{S}_{k,Q\times Q} \cdot \mathbf{H}_{k,Q\times L} + \mathbf{W}_{k,Q\times L}. \tag{15}$$

where $\mathbf{\Lambda}_{k,Q\times Q}$ is diagonal matrix representing the phase rotations of the received demodulated samples due to the presence of sampling frequency offset.

A. Sample Frequency Offset Estimation

If the MIMO-OFDM transmission is being carried out in blocks of Q OFDM symbols, then phase rotation between consecutive blocks of OFDM symbols increases in a linear fashion. Hence let the received sample matrix corresponding to the preamble be given by

$$\mathbf{R}_k^{\text{preamble}} = \mathbf{\Lambda}_k^{\text{preamble}} \cdot \mathbf{S}_k^{\text{preamble}} \cdot \mathbf{H}_k + \mathbf{W}_k. \tag{16}$$

The received sample matrix for the next block of Q OFDM symbols corresponding to the pilot tones is then given by

$$\mathbf{R}_k^p = \exp\left\{\frac{j2\pi Qk\beta(N+G)}{N}\right\} \times \mathbf{\Lambda}_k^{\text{preamble}} \cdot \mathbf{S}_k^p \cdot \mathbf{H}_k + \mathbf{W}_k. \tag{17}$$

If the channel does not change much for $2Q$ consecutive blocks of OFDM symbols as is the case for wireless

$$R_{g,k}^{(l)} = \sum_{q=1}^{Q} \exp\left\{\frac{j2\pi\beta gk(N+G)}{N}\right\} \mathrm{sinc}(\beta k) \times H_{q,k}^{(l)} S_k^{(q)} + W_{k,\text{AWGN}}^{(l)} + W_{k,\text{ICI}} \tag{14}$$

DOCKET ALARM

Explore Litigation Insights

Docket Alarm provides insights to develop a more informed litigation strategy and the peace of mind of knowing you're on top of things.

Real-Time Litigation Alerts

Keep your litigation team up-to-date with **real-time alerts** and advanced team management tools built for the enterprise, all while greatly reducing PACER spend.

Our comprehensive service means we can handle Federal, State, and Administrative courts across the country.

Advanced Docket Research

With over 230 million records, Docket Alarm's cloud-native docket research platform finds what other services can't. Coverage includes Federal, State, plus PTAB, TTAB, ITC and NLRB decisions, all in one place.

Identify arguments that have been successful in the past with full text, pinpoint searching. Link to case law cited within any court document via Fastcase.

Analytics At Your Fingertips

Learn what happened the last time a particular judge, opposing counsel or company faced cases similar to yours.

Advanced out-of-the-box PTAB and TTAB analytics are always at your fingertips.

API

Docket Alarm offers a powerful API (application programming interface) to developers that want to integrate case filings into their apps.

LAW FIRMS
Build custom dashboards for your attorneys and clients with live data direct from the court.

Automate many repetitive legal tasks like conflict checks, document management, and marketing.

FINANCIAL INSTITUTIONS
Litigation and bankruptcy checks for companies and debtors.

E-DISCOVERY AND LEGAL VENDORS
Sync your system to PACER to automate legal marketing.